Dissipative phase transition in a mirrorless optical parametric oscillator

Sushree S. Sahoo [1,2,*] Satya S. Nayak,[1,3] Soumya R. Mishra,[1] and Ashok K. Mohapatra [1,†]

[1]*National Institute of Science Education and Research Bhubaneswar, HBNI, Jatni-752050, India*
[2]*TIFR Centre for Interdisciplinary Sciences, Tata Institute of Fundamental Research, Hyderabad-500017, India*
[3]*Variable Energy Cyclotron Centre, 1/AF Bidhannagar, Kolkata-700064, India*

We experimentally demonstrate a dissipative phase transition in a mirrorless optical parametric oscillator (MOPO) using a double-Λ system in thermal atomic vapor. Bistable behavior is observed in the output power of the beams generated via the MOPO with the variation of the input power of the driving fields. We show that the long-lived hyperfine ground-state coherence induced by the Gaussian pump and the generated fields leads to the observation of optical bistability in the MOPO threshold. We further study the critical slowing-down of nonequilibrium dynamics in the vicinity of the forward threshold where the switching time of the generated fields diverges with the critical exponent, $\alpha = -0.86 \pm 0.02$. Our observations pave the way to understanding and characterizing the phase transitions in driven-dissipative systems using a simple nonlinear optical system like the MOPO.

I. INTRODUCTION

Dissipation in quantum many-body systems is inevitable due to their interaction with the environment. When the system is externally driven by a coherent source, the interplay between driving and dissipation leads the system to a steady state far from equillibrium. Unlike systems at thermal equilibrium, phase transitions in such driven-dissipative quantum systems known as dissipative phase transitions (DPTs) are far less understood. Recent advancements in experimental tools and techniques have allowed investigations of DPTs using different systems such as Bose-Einstein condensate coupling to an optical cavity [1,2] or a semiconductor microcavity [3,4] and Rydberg excitation in dilute atomic vapor [5]. In parallel, few theoretical models have also been developed to understand and characterize the DPT [6–14]. One of the intriguing features associated with DPTs is optical bistability, which is the coexistence of two stable phases differing in their optical properties [15]. Typically, a bistable system consists of a nonlinear medium placed inside a cavity to provide optical feedback to the system [16]. However, there are instances of optical bistability in systems without the requirement for a resonator such as bistability using degenerate four-wave mixing [17], intrinsic atom-light coupling [18], polarization bistability in sodium vapor [19], resonatorless bistability with single-mirror feedback [20], dynamic bistability in Raman generation [21], or bistability as a result of cooperative interatomic interaction with Rydberg atoms [5].

In this paper, we report the observation of optical bistability at the threshold of a mirrorless optical parametric oscillator (MOPO) using a double-Λ system in thermal atomic vapor [22]. A MOPO is the nonlinear interaction of a counter-propagating pump and control fields leading to the parametric oscillation of a pair of counter-propagating Stokes and anti-Stokes fields in the absence of a cavity [23]. The existing works on MOPOs are mostly centered on the study of its narrow linewidth [24,25], tunable threshold [26], and spatial correlation [22]. We observe that the generated Stokes and anti-Stokes power display bistable behavior with variation of the input power of the driving fields, which is further explained using a suitable theoretical model. We also present experimental evidence that the hyperfine ground-state coherence or the spin waves [27–29] induced by interactions of the pump (control) and generated Stokes (anti-Stokes) fields with the medium lead to bistable behavior of the MOPO threshold. The observed optical bistability in MOPOs is associated with the first-order phase transition, with spin waves serving as the order parameter. The memory effect due to the finite lifetime of the spin waves makes it an ideal system for the investigation and better understanding of the DPT. Here, we demonstrate the critical slowing-down of the nonequilibrium dynamics by measuring the response of the system in the vicinity of the MOPO threshold.

II. THEORETICAL MODEL

Figure 1(a) shows a schematic of the energy level diagram for the MOPO process. To understand the MOPO-based bistability, we consider the propagation equations of the Stokes and the anti-Stokes beams inside the medium. Under slowly varying amplitude approximation for the case of plane waves, while neglecting the effect of cross-phase modulation, the nonlinear wave equations can be written as [30,31]

$$\frac{d\Omega_s}{dz} = -3ik\left(\frac{N\mu^2}{\epsilon_0\hbar}\right)\frac{\Omega_p}{2\Delta_p}\rho_{12}^{(ca)}, \qquad (1)$$

$$\frac{d\Omega_a}{dz} = -3ik\left(\frac{N\mu^2}{\epsilon_0\hbar}\right)\frac{\Omega_c}{2\Delta_c}\rho_{21}^{(ps)}, \qquad (2)$$
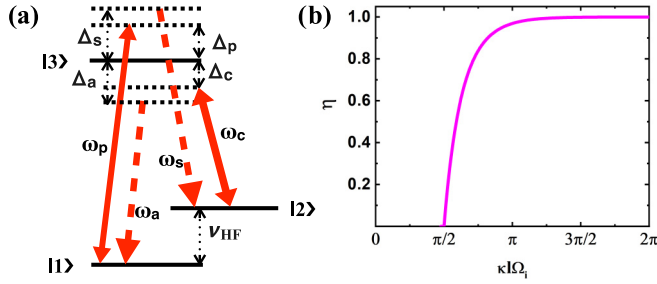
*sushree.ss@niser.ac.in
†a.mohapatra@niser.ac.in

FIG. 1. (a) Schematic of the energy level diagram for the MOPO process. ν_{HF} is the splitting of the hyperfine ground states $|1\rangle$ and $|2\rangle$, whereas $|3\rangle$ is the excited state. ω_p (ω_c) represents the optical frequency of the input pump (control) beam and ω_s (ω_a) corresponds to the optical frequency of the generated Stokes (anti-Stokes) beam. Δ_p (Δ_c) is the single-photon detuning of the pump (control) beam and Δ_s (Δ_a) is the single-photon detuning of the Stokes (anti-Stokes) beam. (b) Variation of the pump conversion efficiency (η) with different values of $\kappa l \Omega_i$ showing the threshold of MOPO generation at $\kappa l \Omega_i = \frac{\pi}{2}$.

where Ω_p (Ω_s) and Ω_c (Ω_a) are the Rabi frequencies of the pump (Stokes) and control (anti-Stokes) beams, respectively. k denotes the magnitude of the wave vector and is taken to be the same for both Stokes and anti-Stokes beams. N is the number density of the atomic vapor. $\rho_{21}^{(ps)} = \Omega_p \Omega_s / (4\Delta_p(\Delta_{eff} - i\gamma_c))$ ($\rho_{12}^{(ca)} = \Omega_c \Omega_a / (4\Delta_c(\Delta_{eff} + i\gamma_c))$) is the ground-state coherence induced by the interaction of pump (control) and Stokes (anti-Stokes) beams. $\Delta_{eff} = \Delta - \Omega_p^2/(4\Delta_p) + \Omega_s^2/(4\Delta_p) + \Omega_c^2/(4\Delta_c) - \Omega_a^2/(4\Delta_c)$ with $\Delta = \Delta_s - \Delta_p = \Delta_a - \Delta_c$ and γ_c is the dephasing rate of the ground-state coherence. We consider the generation with effective detuning, $\Delta_{eff} = 0$ [32]. Here, we have neglected the absorption for all beams due to their large detunings from the corresponding transitions. As the control conversion efficiency is negligibly low, the control beam can be considered undepleted. However, the pump depletion is taken into account by considering $\Omega_p^2(z) + \Omega_s^2(z) = \Omega_p^2(z=0) = \Omega_i^2$, where Ω_i is the input pump Rabi frequency. We use the boundary conditions, $\Omega_s^2(z) + \Omega_a^2(z) = \Omega_s^2(z=l) = \Omega_s^2(z=0) = \Omega_0^2$, where l is the length of the vapor cell. It is to be noted that Ω_0 is the Rabi frequency of the generated Stokes field. Now, Eqs. (1) and (2) can be simplified to get

$$\frac{d^2\Omega_s}{dz^2} + \kappa^2(\Omega_i^2 + \Omega_0^2)\Omega_s - 2\kappa^2\Omega_s^3 = 0. \quad (3)$$

Here, $\kappa = -\frac{3}{8}k(\frac{N\mu^2}{\epsilon_0\hbar})\frac{\Omega_c}{\Delta_p\Delta_c\gamma_c}$. With a change of variables, $\Omega_s \to x$ and $z \to t$, Eq. (3) resembles the equation of motion of a classical particle under the action of a potential given by $V(x) = \frac{1}{2}\kappa^2(\Omega_i^2 + \Omega_0^2)x^2 - \frac{1}{2}\kappa^2 x^4$. The solution of Eq. (3) that meets the boundary conditions is found to be $\kappa l \Omega_i = \text{EllipticK}(\eta)$ [33]. Here, η stands for the pump conversion efficiency, given as $\eta = \Omega_0^2/\Omega_i^2$. The value of η can be evaluated for the given Ω_i, κ, and l and the threshold condition for the system is defined for $\eta \to 0$ as shown in Fig. 1(b). Hence Eq. (3) has a solution with a positive η if $\kappa l \Omega_i > \frac{\pi}{2}$. The threshold Rabi frequency of the pump field for the plane-wave case is given as $\frac{\pi}{2\kappa l}$, which is consistent with the reported threshold condition for similar systems [25,26].

For a medium with thermal vapor, the dephasing rate is dominated by the transit time of the atoms through the beam and is given as $\gamma_c = v_{avg}/2r$, where v_{avg} is the average velocity of the atoms and r is the radius of the beam in the transverse direction. The threshold condition can now be rewritten by considering the r dependence as

$$\kappa_0 l \Omega_i r = \frac{\pi}{2},$$

where $\kappa_0 r = \kappa$. In the above model, the pump beam is considered to be a cylinder with radius r and the Rabi frequency is constant in the transverse direction. However, in the case of a Gaussian pump beam with $1/e-$radius being w_o, the spatial dependence of the Rabi frequency in the transverse direction is $\Omega_i(r) = \Omega_m e^{-r^2/2w_0^2}$, where Ω_m is the Rabi frequency at the center of the beam. The threshold condition for the Gaussian beam can be modified as $\kappa_0 l \Omega_m e^{-r^2/2w_0^2} r = \pi/2$. Since $e^{-r^2/2w_0^2}r$ has a maximum value of $w_o/\sqrt{e}$, the above equation does not have a solution for $\Omega_m < \Omega_F$, where $\Omega_F = (\frac{\pi}{2\kappa_0 l})(\frac{\sqrt{e}}{w_0})$, and it is denoted as the forward threshold Rabi frequency of the MOPO for a Gaussian pump beam.

The forward threshold Rabi frequency for the case of a Gaussian beam is much larger than the threshold for the case of a plane wave, which leads to an abrupt generation of the MOPO at the center of the beam. Now, the backward threshold is a consequence of the long-lived ground-state atomic coherence present in the system, which remains even if the pump power is decreased to a value lower than the initial forward threshold. This finite atomic coherence in the backward direction is determined by the size of the Stokes beam. When the pump peak power is reduced to a value such that the size of the Stokes beam is insufficient to sustain coherence throughout the medium, then the Stokes power falls to 0, resulting in the backward threshold. So, the backward threshold can be determined by replacing r with w_s in the equation for the threshold condition and is given as $\Omega_B = (\frac{\pi}{2\kappa_0 l})(\frac{1}{w_s})$. The condition $w_s > w_o/\sqrt{e}$ implies $\Omega_F > \Omega_B$, which leads to the bistability as observed in the system.

III. EXPERIMENTAL METHODS AND RESULTS

A schematic of the experimental setup is shown in Fig. 2(a). The input pump and control beams are derived from two lasers operating at 780 nm (D2 line of rubidium) and counter-propagating to each other in a magnetically shielded 5-cm Rb vapor cell heated to 115 °C (atomic density, $\sim1.5 \times 10^{13}$ cm^{-3}). The pump beam is ~1.2 GHz blue-detuned to the transition ^{85}Rb $F = 2 \to F' = 3$ and the control laser is red-detuned to the ^{85}Rb $F = 3 \to F' = 4$ transition by ~800 MHz. We use a lens combination to vary the pump beam size, whereas the control beam waist is fixed at 1 mm. The input beams are linearly polarized in the same direction, whereas the generated beams are cross-polarized to the input beams and hence are filtered using polarizing beam splitters. The details of the experimental setup and the optimized parameters to achieve the single spatial and temporal mode in the MOPO can be found in Ref. [22]. To experimentally study MOPO-based optical bistability, the control power is fixed above the threshold value and the pump power is modulated with a ramp function using an acousto-optic modulator. In this
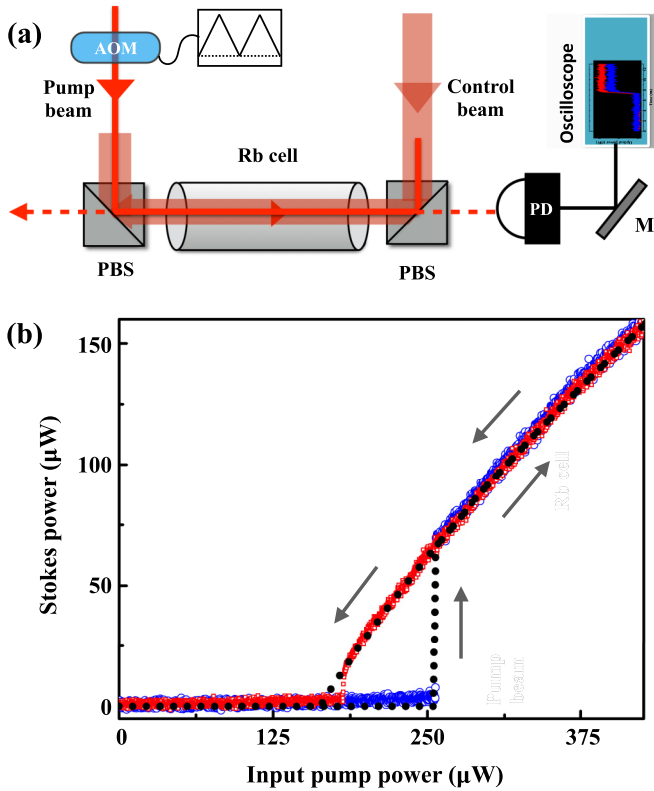
FIG. 2. (a) Schematic of the experimental setup for the observation of MOPO-based optical bistability. PBS, polarizing beam splitter; AOM, acousto-optics modulator; PD, photodetector. (b) Bistability of the Stokes power with pump power variation, where $w_0 = 150 \, \mu$m and the control power is fixed at 45 mW. Open blue circles (open red squares) show the experimental data in the increasing (decreasing) pump power direction and also represented by the arrows. Filled black circles represent the theoretical fitting. The fitting parameters are $\kappa = -6.3 \times 10^{-7}$ m^{-1} s, $l = 0.05$ m, and $w_s = 113 \, \mu$m.

way, we study the pump threshold in both the increasing and the decreasing directions of the pump power. The generated Stokes power is detected using a photodetector and is analyzed using an oscilloscope.

The long-lived coherence between the ground states of the system is one of the reasons for the observation of bistability. Hence, both threshold values depend on the frequency of the ramp signal used to change the pump power. This observation is similar to the dynamical bistability observed in a Raman gain system using alkali vapor [21]. However, as we further study the system with a reduced modulation frequency, below 50 Hz, the thresholds are observed to be independent of the modulation frequency. In this regime, the change in pump power is sufficiently slow that the system always remains in steady state. The steady-state bistability observed in our system is fundamentally different from the dynamical bistability, which vanishes at a slower modulation frequency [21]. At steady state, we observe that the pump threshold value for the MOPO in the increasing pump power direction is larger than the value in the decreasing pump power direction as shown in Fig. 2(b). We also theoretically evaluate the generated Stokes power ($\propto \Omega_0^2$) using the model presented in the text. The Rabi

frequency of the pump is calculated as $\Omega_m = \Gamma \sqrt{\frac{P}{\pi w_0^2} / (2I_{sat})}$, where I_{sat} and Γ are the saturation intensity and excited-state decay rate of ^{85}Rb, respectively. P denotes the power of the beam. We first calculate the generated Stokes power in the direction of decreasing pump power by considering the pump beam as a plane wave. γ_c is determined from the Stokes beam size, which is measured using $4f$ imaging of the Stokes and anti-Stokes beams at both exit faces of the cell [22]. It is found that the Stokes beam size varies in the range of 100–125 μm over the length of the cell but is independent of the pump beam power in the range of single-mode MOPO generation except near the backward threshold power. The calculated Stokes power is then fitted with the experimental data by adjusting the value of κ and an overall gain factor to account for any loss of the pump and Stokes power while propagating through the cell and different optical elements to the detector. The forward threshold is further calculated using the relation $\Omega_F / \Omega_B = \sqrt{e} w_s / w_0$, where the beam sizes used are $w_0 = 150 \, \mu$m and $w_s = 113 \, \mu$m. Our theoretical model fits well with the experimental observation as shown in Fig. 2(b).

To verify the effect of the long-lived atomic coherence in the system, we perform an experiment by modulating the input pump power following a functional form as shown in Fig. 3(a). The pump is switched on by keeping its power above the forward threshold (power level A) such that Stokes and anti-Stokes beams are generated. Then the pump power is switched to the bistable region (level B). While the system is in the bistable region, the pump is switched off completely for a short period of ΔT to study the MOPO generation. The corresponding generated Stokes power is shown in Fig. 3(a). Initially, the pump power is efficiently converted to Stokes power at both level A and level B. As the pump power is switched to 0 in the bistable region, the Stokes generation stops. Now as the pump power is switched back to level B, which is lower than the forward threshold, the Stokes beam is observed to be generated after a delay as depicted in the inset in Fig. 3(a). This switching-back of the Stokes power is evidence of the presence of finite ground-state coherence in the bistable regime, which leads to generation of the Stokes beam. We also observe that as we increase ΔT, after a certain value, the Stokes beam is not switched back as a result of complete decay of the coherence. The coherence time in this system is then defined as the maximum value of ΔT, for which the Stokes beam is switched back to a finite value. We measure this coherence time in the bistable region as a variation of the pump beam waist. The corresponding experimental data are presented in Fig. 3(b), where the coherence time is found to depend linearly on the beam waist. This behavior follows the fact that atomic coherence is limited by the transit time of the atoms through the laser beam.

As is well known, optical bistability is a characteristic feature of the first-order phase transition [34]. For our case, the experimental observation of a discontinuity in the generated field at the threshold and the bistable behavior imply the presence of a first-order phase transition, where the ground-state coherence acts as the order parameter. To investigate the nonequilibrium dynamics of the phase transition, the input pump power is switched on from 0 to a finite value, which
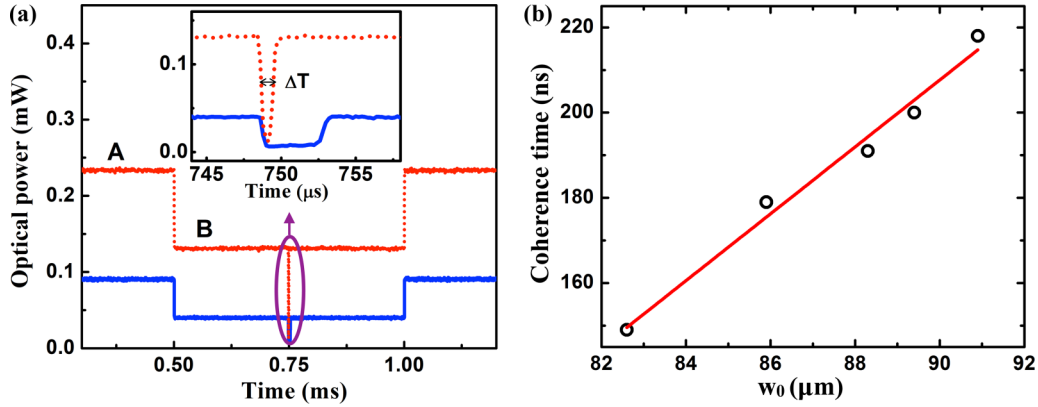
FIG. 3. Experimental verification of the role of atomic coherence for optical bistability. (a) Stokes power (solid blue line) measured by the response to pump power modulation (dotted red line). Level *A* refers to the pump power above the forward threshold and level *B* falls within the bistable region. Inset: Expansion of the highlighted area in (a) with a ΔT value of 0.8 μs. (b) Variation of coherence time with the pump beam waist (w_0). Black circles represent experimental data and the solid red line shows the linear fitting.

is higher than the forward threshold power, and the Stokes beam is generated with a time delay called the switch-on time (τ). The inset in Fig. 4(a) shows the experimental data for the delayed Stokes power generation in response to a pulsed pump beam. As the pump power approaches the threshold value, the switch-on time of Stokes generation diverges (critical slowing-down). We observe that τ follows a power law given by $\tau = A(P - P_T)^\alpha$, where P is the input pump power, P_T is the threshold power, and α is the critical exponent. The experimental data are shown in Fig. 4(a), where the value of α is evaluated from the fitting. For a system exhibiting optical bistability in an optical cavity, the value of the critical exponent (α) is predicted to be -0.5 [35,36]. The measured critical exponent for the system with an optical cavity [37] as well as the Rydberg system [5] is found to be consistent with the theoretical prediction. On the other hand, the value of α for this system is found to be -0.86 ± 0.02, which is evaluated for a wide range of experimental parameters such as different control powers and atomic densities as presented in Fig. 4(b).

IV. SUMMARY AND CONCLUSION

In summary, we have demonstrated a DPT using a simple nonlinear optical system like the MOPO. Compared to systems with an optical cavity, this system exhibits a conventionally different nonequilibrium phase transition with a different value of the critical exponent. Also, MOPO-based optical bistability is observed when the Gaussian pump field is used to drive the system. The theoretical model predicts that if the pump field is a plane wave, then the MOPO will have a laserlike threshold, which is associated with a second-order phase transition. Since the MOPO threshold strongly depends on the transverse profile of the pump field, which can easily be modulated using a spatial light modulator, it can offer a very rich system to study and investigate different aspects of the DPT.
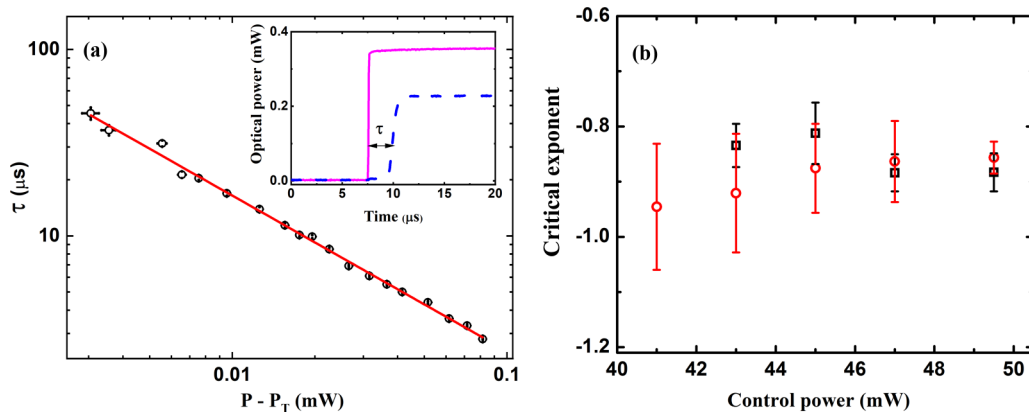
FIG. 4. (a) Variation of the switch-on time (τ) of Stokes beam generation with the input pump power. Inset: Output Stokes power (dotted blue line) in response to input pump pulse (solid magenta line). (b) Critical exponent (α) measured with different control powers. Open red circles (open black squares) represent the data corresponding to an Rb vapor density of 8.2×10^{12} cm^{-3} (1.5×10^{13} cm^{-3}).

[1] K. Baumann, C. Guerlin, F. Brennecke, and T. Esslinger, Nature **464**, 1301 (2010).

[2] J. Klinder, H. Keßler, M. Wolke, Ludwig Mathey, and A. Hemmerich, Proc. Natl. Acad. Sci. USA **112**, 3290 (2015).

[3] S. R. K. Rodriguez, W. Casteels, F. Storme, N. Carlon Zambon, I. Sagnes, L. Le Gratiet, E. Galopin, A. Lemaître, A. Amo, C. Ciuti, and J. Bloch, Phys. Rev. Lett. **118**, 247402 (2017).

[4] T. Fink, A. Schade, S. Höfling, C. Schneider, and A. Imamoglu, Nat. Phys. **14**, 365 (2018).

[5] C. Carr, R. Ritter, C. G. Wade, C. S. Adams, and K. J. Weatherill, Phys. Rev. Lett. **111**, 113901 (2013).

[6] S. Diehl, A. Micheli, A. Kantian, B. Kraus, H. P. Buechler, and P. Zoller, Nat. Phys. **4**, 878 (2008).

[7] S. Diehl, A. Tomadin, A. Micheli, R. Fazio, and P. Zoller, Phys. Rev. Lett. **105**, 015702 (2010).

[8] P. Strack and S. Sachdev, Phys. Rev. Lett. **107**, 277202 (2011).

[9] V. M. Bastidas, C. Emary, B. Regler, and T. Brandes, Phys. Rev. Lett. **108**, 043003 (2012).

[10] E. M. Kessler, G. Giedke, A. Imamoglu, S. F. Yelin, M. D. Lukin, and J. I. Cirac, Phys. Rev. A **86**, 012116 (2012).

[11] L. M. Sieberer, S. D. Huber, E. Altman, and S. Diehl, Phys. Rev. Lett. **110**, 195301 (2013).

[12] W. Casteels, F. Storme, A. Le Boité, and C. Ciuti, Phys. Rev. A **93**, 033824 (2016).

[13] W. Casteels, R. Fazio, and C. Ciuti, Phys. Rev. A **95**, 012128 (2017).

[14] M. Soriente, R. Chitra, and O. Zilberberg, Phys. Rev. A **101**, 023823 (2020).

[15] H. M. Gibbs, *Optical Bistability: Controlling Light with Light* (Academic Press, New York, 1985).

[16] H. M. Gibbs, S. L. McCall, and T. N. C. Venkatesan, Phys. Rev. Lett. **36**, 1135 (1976).

[17] H. G. Winful and J. H. Marburger, Appl. Phys. Lett. **36**, 613 (1980).

[18] D. A. B. Miller, A. C. Gossard, and W. Wiegmann, Opt. Lett. **9**, 162 (1981).

[19] D. J. Gauthier, M. S. Malcuit, A. L. Gaeta, and R. W. Boyd, Phys. Rev. Lett. **64**, 1721 (1990).

[20] T. Ackemann, A. Heuer, Yu. A. Logvin, and W. Lange, Phys. Rev. A **56**, 2321 (1997).

[21] I. Novikova, A. S. Zibrov, D. F. Phillips, A. Andre, and R. L. Walsworth, Phys. Rev. A **69**, 061802(R) (2004).

[22] S. S. Sahoo and S. S. Pati, and A. K. Mohapatra, Phys. Rev. A **98**, 063838 (2018).

[23] A. S. Zibrov, M. D. Lukin, and M. O. Scully, Phys. Rev. Lett. **83**, 4049 (1999).

[24] M. Fleischhauer, M. D. Lukin, A. B. Matsko, and M. O. Scully, Phys. Rev. Lett. **84**, 3558 (2000).

[25] D. A. Braje, V. Balic, S. Goda, G. Y. Yin, and S. E. Harris, Phys. Rev. Lett. **93**, 183601 (2004).

[26] Y. Mei, X. Guo, L. Zhao, and S. Du, Phys. Rev. Lett. **119**, 150406 (2017).

[27] L.-M. Duan, M. D. Lukin, J. I. Cirac, and P. Zoller, Nature **414**, 413 (2001).

[28] Z. Y. Ou, Phys. Rev. A **78**, 023819 (2008).

[29] K. Zhang, J.n Guo, C.-H. Yuan, L. Q. Chen, C. Bian, B. Chen, Z. Y. Ou, and W. Zhang, Phys. Rev. A **89**, 063826 (2014).

[30] M. Jain, H. Xia, G. Y. Yin, A. J. Merriam, and S. E. Harris, Phys. Rev. Lett. **77**, 4326 (1996).

[31] A. J. Merriam, S. J. Sharpe, M. Shverdin, D. Manuszak, G. Y. Yin, and S. E. Harris, Phys. Rev. Lett. **84**, 5308 (2000).

[32] The beat signal between the pump and the Stokes beam, which is given by $\omega_s - \omega_p = \nu_{HF} - \Delta_{eff}$, is experimentally investigated. We find that the beat signal has a linewidth of $\sim$14 kHz and its frequency is measured to be $3.035\,73 \pm 0.000\,35$ GHz. Here, 3.035 73 GHz is the hyperfine splitting between ^{85}Rb $5\,^2S_{1/2} F = 2$ and $F = 3$ states. Hence, Δ_{eff} varies by $\sim$700 kHz, while the width of the Stokes transmission signal is $\sim$5 MHz in the single-mode MOPO regime [22]. Therefore, Δ_{eff} can be considered to be constant, and here we have considered Δ_{eff} to be 0 for the simplicity of the calculation.

[33] The function EllipticK refers to the complete elliptic integral of the first kind and is defined as, EllipticK $(x) = \frac{\pi}{2}(1 + \frac{x}{4} + \frac{9x^2}{64} + \frac{25x^3}{128} + O(4))$.

[34] C. M. Bowden and C. C. Sung, Phys. Rev. A **19**, 2392 (1979).

[35] G. Grynberg and S. Cribier, J. Physique Lett. **44**, 449 (1983).

[36] P.-H. Tsao and W.-C. Liu, Modern Phys. Lett. B **06**, 359 (1992).

[37] S. Cribier, E. Giacobino, and G. Grynberg, Opt. Commun. **47**, 170 (1983).